Bulk and Mapping Speciation Analyses Unveil the Pattern and Heterogeneity of Cu Species during Organic Waste Treatment

Emmanuel Doelsch, Maureen Le Bars, Barbara Etschmann, Thiago Formentini, Samuel Legros, Clément Levard, Perrine Chaurand, Isabelle Basile-Doelsch, Jérôme Rose, Gianluca Brunetti, et al.

Bulk and Mapping Speciation Analyses Unveil the Pattern and Heterogeneity of Cu Species during Organic Waste Treatment

Emmanuel Doelsch

Maureen Le Bars

Barbara Etschmann

Thiago Formentini

Samuel Legros

Clément Levard

Isabelle Basile Doelsch

Jérôme Rose

Gianluca Brunetti

Casey Doolette

Daryl Howard

Enzo Lombi

Graphical abstract

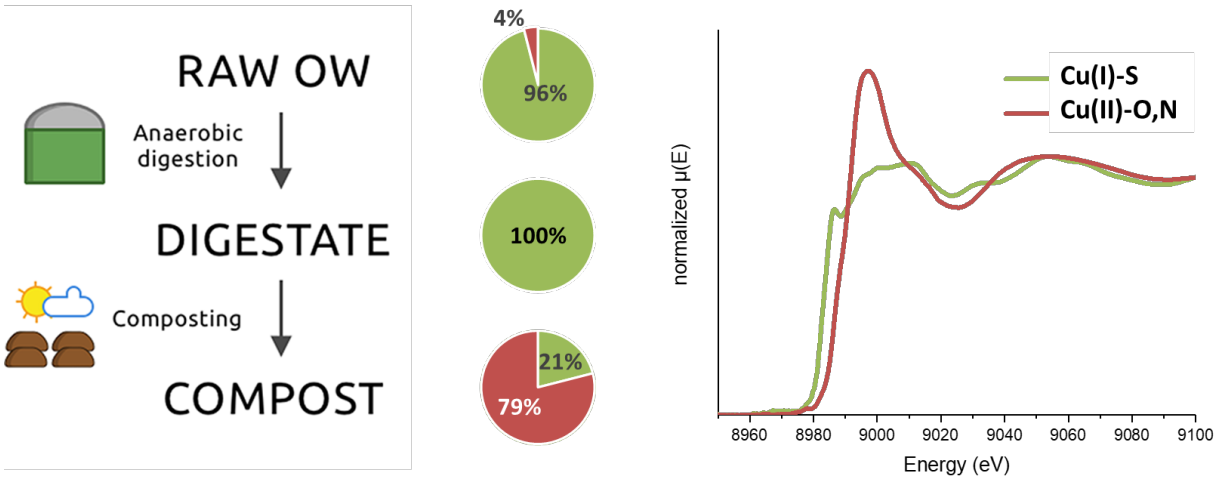

Abstract

Introduction

Organic wastes (OWs) such as livestock manure, sewage sludge, and industrial residues are the most important sources of Cu contamination to agricultural soils. In the early 2000s, they accounted for 56%, 58% and 69% of the total Cu inputs to croplands in England and Wales[1], France[2] and China[3] respectively. Nevertheless, assessing the (eco)toxicological impacts of this large inputs requires more than information regarding total concentrations. Bioavailability and chemical speciation are essential factors controlling Cu (eco)toxicity. [4-6] For instance, nanosized CuS showed stronger toxicity relative to nano-CuO in medaka embryos due to elevated free Cu ions released from nano-CuS, leading to significant increase in oxidative stress and causing toxicity in embryos. [7] However, assessing the chemical forms of contaminants occurring at trace levels in complex matrices remains an analytical challenge. Indeed, OWs are heterogeneous media with varying composition, pH, oxidation reduction potential, and dry matter content that highly affect trace metal speciation. In addition, OWs are usually subjected to different storage and treatment processes that can alter physical-chemical conditions and hence the Cu speciation.

Most studies assessing the Cu speciation in OWs focused on only one type of OW and contrasted Cu species were identified. Cu-sulfides were detected in pig slurry[8, 9] and fresh biosolids[10]; Cu-sulfides and Cu bound to organic matter (or phosphate) were present in fresh broiler excreta[11], and stockpiled biosolid [10, 12]; whereas Cu bound to organic matter was identified in compost produced from organic fraction of municipal or household wastes.[13] These isolated findings do not allow to determine whether the OW origin (*i.e.* agricultural, urban) influences copper speciation or whether treatment (e.g. composting) alters the initial speciation of the raw OW. The impact of the treatment on Cu speciation pattern has been mainly assessed at laboratory scale : anaerobic digestion[14], anaerobic digestion combined with hydrothermal treatment[15], incineration[16] pyrolysis.[17] As laboratory conditions cannot always fully represent full-scale site conditions (e.g., hydraulic retention time, storage conditions), knowledge of Cu speciation pattern in full-scale treatment plants is therefore essential. In addition, no study to date investigated the transformations in Cu speciation by considering OWs deriving from different sources commonly applied to agricultural soils: agricultural wastes, urban wastes, and industrial wastes.

The studies reviewed above have mainly relied on X-ray absorption spectroscopy (XAS). XAS analysis can be equally applied to solid and liquid samples and provide relevant information about the oxidation state, symmetry, identity of the coordinating ligand and more distant neighbouring atoms allowing to characterize the complete molecular environment of the element of interest.[18] The standard bulk XAS techniques probe a volume of a few mm^3 and thus provide an average global response regarding Cu speciation. This often limits the information that can be acquired. Indeed, Cu speciation may vary within micrometer to submicrometer regions,[19] posing methodological challenges when investigating biogeochemical processes.[20] In recent years, the development of laterally resolved synchrotron techniques combined with fast fluorescence detector systems have provided new opportunities to address the issue of the speciation heterogeneity at a micrometer spatial scale.[18, 21] It is now possible to collect an image with an X-ray absorption near edge structure spectroscopy (XANES) spectrum recorded at each pixel, which has opened the door to speciation mapping for elements at low concentrations. This so-called XANES imaging approach has been successfully tested with biosolids[22] and confirmed that Cu speciation and distribution were affected by stockpiling.[10] However, these findings and analytical approach need to be tested for a larger series of OWs with different characteristics.

Here we conducted a comprehensive study to systematically investigate the speciation of Cu in raw and treated OWs sampled in six different full-scale OW treatment plants chosen to represent (i) the common sources of OW (agricultural, urban, and industrial) and (ii) the common processes used for

treating these OWs (anaerobic digestion and composting). Standard bulk XAS analysis was first used to investigate the overall impact of OW origin and treatment on the speciation of Cu. Subsequently, we explored the spatial heterogeneity of Cu species in OWs at the micrometer scale to identify minor species (i.e. individually contributing to less than 10% of the total spectra) which cannot be assessed using standard methods.

Material and methods

Organic waste samples. Six different full-scale treatment plants were selected to represent the three most common types of raw OW used as feedstock for anaerobic digestion (AD) and composting: Urban (sewage sludge), Agri (agricultural waste: livestock effluents, crop residues, etc.), and Central (mix of different types of OW digested in a centralized plant). OW was sampled just before AD (samples called "raw OW") and just after AD ("digestate"). When a digestate post-treatment was included in the process, the intermediate and the final products were sampled (solid/liquid fractions of digestate called "solid digestate" and "liquid digestate" respectively, "pellets" and "compost"). At the composting plant (Urban-3), OW was sampled before ("raw OW") and after composting ("compost"). At each plant, around 3 kg of dry matter (DM) of OWs were sampled. All the samples were frozen at −20 °C, at the latest 3 days after on-site sampling. The composition of the raw OWs and the different steps of the treatment that were sampled are reported in Table SI-1. A more complete description of the treatment plants, the physical-chemical analyses and characteristics of the raw and treated OWs can be found elsewhere. [23]

Standard bulk XAS analysis. Cu K-edge XAS spectra were recorded at the ESRF synchrotron (Grenoble, France) on the BM30B (FAME) beamline, at the SSRL (Stanford, USA) on the 11−2 beamline and at the Australian synchrotron (Melbourne, Australia) on the XAS beamline. To avoid Cu speciation changes during OWs storage before XAS analysis a specific sample preparation was implemented.[23] OWs previously frozen were freeze dried, cryo-grounded (Retsch MM400), pressed into pellets and stored at −20 °C until XAS analysis. Spectra acquisition was performed at liquid helium temperature to prevent X-ray sample damage. Spectra for each sample was the average of at least three scans, depending on the Cu concentration and the signal-to-noise ratio. Each scan was focused on a different specimen position to reduce the risk of beam damage and obtain representative spectra. Measurements were carried out in fluorescence mode with a 30- or a 100-element solid-state Ge detector for OWs and in transmission mode for the references compounds. Energy calibration was performed using metallic Cu reference foil (absorption edge defined at 8979 eV). Normalization and data reduction were performed according to standard methods[24] using Fastosh[25] and Athena[26] softwares. Both regions of the XAS spectra were analysed to reveal complementary information: X-ray absorption near edge structure spectroscopy (XANES) for oxidation state, three-dimensional geometry, and coordination environment of Cu and extended X-ray absorption fine structure spectroscopy (EXAFS) for identification of the Cu bearing phases. The fitting procedure of Cu XANES and EXAFS spectra was based on a combination of principal component analysis (PCA), target transformation (TT), and linear combination fitting (LCF). Details on PCA, TT, and LCF results are given in SI-2 for XANES, SI-3 for EXAFS. Details on synthesis and characteristics of nano-CuS and amorphous Cu phosphate reference compounds are provided in SI-4. The complete Cu reference compound library is shown in SI-4 and described in previously published studies.[9, 11, 13, 14, 27-30]

XANES imaging analysis. Cu K-edge XANES imaging were recorded at the Australian synchrotron on the X-ray Fluorescence Microscopy beamline. The beamline is equipped with a Kirkpatrick-Baez mirrors to focus the beam and the 384-element MAIA detector which combines high count-rate capacity and 'on the fly' scanning mode. [31] The XANES imaging analysis was conducted on seven OWs, selected to represent the three types of raw OW (urban, agri and central), the two types of treatment (AD and composting). Freeze-dried and cryo-grounded OWs were gamma sterilised before analyses to comply with Australian quarantine regulation. A subsample of each OW was thinly dispensed on kapton tape and mounted on the sample holder immediately before the analysis performed at room temperature.

An initial large area survey scan of 7x4 mm for raw and compost from Urban-3 or of 8x2 mm for raw and treated OWs from Agri-1 and Central-1 was collected at 15.8 keV to reveal the overall elemental distribution. Subsequently, a smaller area of interest (5x0.22 mm for raw and compost from Urban-3 or of 3x0.2 mm for raw and treated OWs from Agri-1 and Central-1) was chosen to conduct XANES imaging (XANES stack) consisting of 95 individual maps collected at increasing incident energies from 8900 eV to 9300 eV across the Cu K-edge. Energies were selected as follows: 8900–8960 eV in 10 eV increments, 8970–8975 eV in 1 eV increments, 8976–8999.5 eV in 0.5 eV in increments, 9000–9009 eV in 1 eV increments, 9010– 9046 eV in 4 eV increments, 9050–9090 eV in 10 eV increments, and 9100-9300 in 25 eV increments. XANES maps were collected with a 1 ms dwell time and 2 µm steps using a motorised sample stage, and a micro-focussed X-ray beam to a spot size of 2 µm. XANES stack contained 275 000 pixels for raw and compost from Urban-3 or 150 000 pixels for raw and treated OWs from Agri-1 and Central-1 and 95 energies per pixel. Individual XANES maps were extracted as TIFF files from GeoPIXE™ and were imported into ImageJ v1.53 to be converted into a stack of TIFF images. This stack was then imported into Mantis 3.1.12[32] where PCA followed by cluster analysis were applied. [33, 34] PCA was used to find a reduced set of eigenspectra and cluster analysis was used to group spectroscopically similar pixels together. The average XANES spectra from each cluster were further analysed by LCF using the Athena software (SI-4).

Results and discussion

Copper concentrations in OWs

The Cu concentration in the OWs ranged from 64 to 385 mg.kg^{-1} of dry matter (Figure 1a). OWs of urban origin (*i.e.* raw, digestate and compost of sewage sludge) were richer in Cu (mean concentration = 266 ± 81 mg.kg^{-1}) than OWs of agricultural or central origin (mean concentration = 166 ± 83 mg.kg^{-1}). This is in close agreement with Cu concentrations measured in organic wastes from various origins (urban or agricultural) and from five regions in three countries (Madagascar, Senegal, France) located in temperate or tropical environments.[35] Note that the Cu concentrations in raw urban wastes were lower than the maximum permissible limits for agricultural use in Europe (1 000 to 1 750 mg.kg^{-1} DM), but higher than the most restrictive threshold values set by Netherlands legislation (75 mg.kg^{-1} DM).[36]

After anaerobic digestion, Cu concentrations in the digestates increased compared with the raw waste from which they derived for all plants making use of this treatment, *i.e.* Urban 1, Urban 2, Agri 1, Central 1, and Central 2. This is explained by the loss of an organic carbon portion that is converted into biogas (CO_2 and CH_4) during AD that causes a relative increase in the Cu concentration.[14] Conversely, composting of Urban-1 solid digestate and Urban-2 pellets caused a decrease in Cu concentration (in relation to the solid digestate and pellets) due to dilution caused by the addition of green waste as a co-substrate during the composting process.[37] However, the latter trend was not observed for agriculture-derived OW (Agri-1).

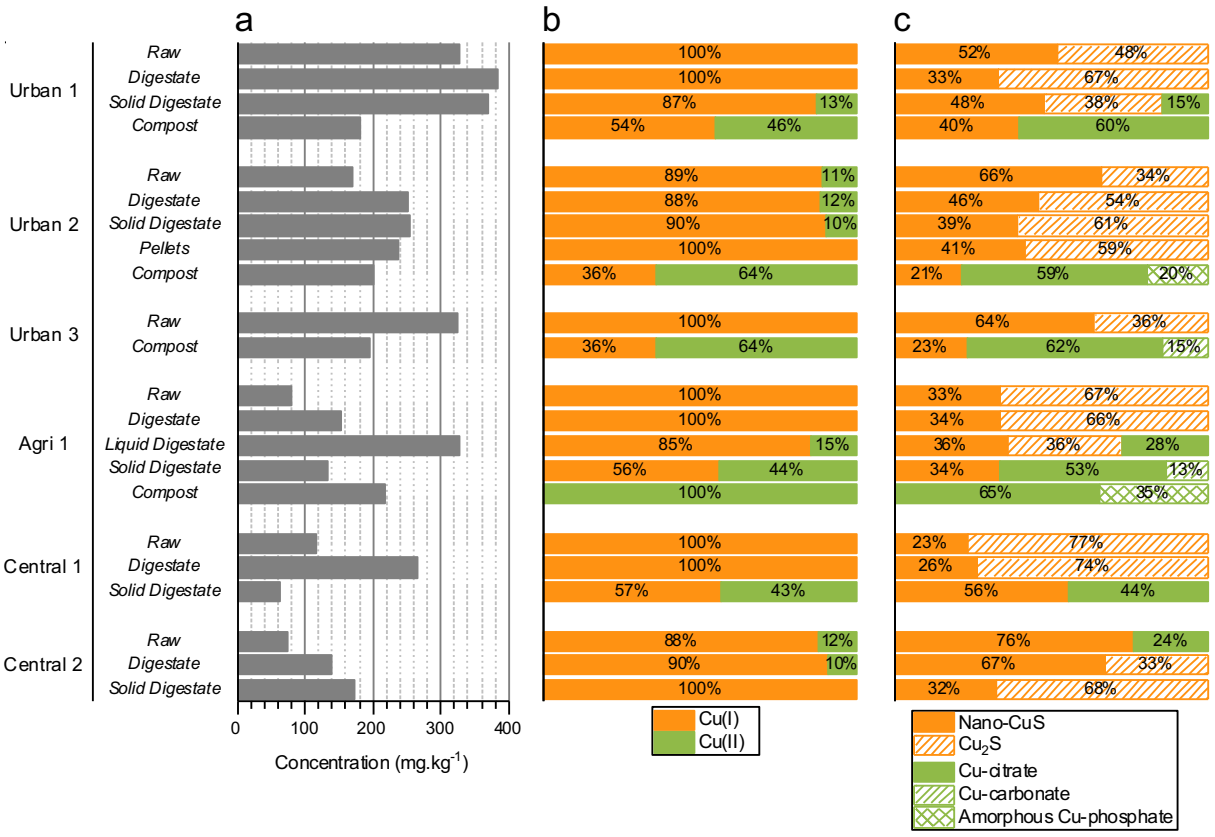

Figure 1: (a) Cu concentration (mg.kg^{-1} of dry matter), (b) oxidation state (LCF of the Cu K-edge XANES spectra), and (c) speciation (LCF of the Cu K-edge EXAFS spectra) for raw and treated OWs.

Changes in Cu oxidation state along OW treatment

The Cu K-edge XANES spectra for raw and treated OWs at different steps of the treatment at the Agri-1 site in comparison to the spectra of Cu(I) (nano-CuS) and Cu(II) (Cu-malate) reference compounds are reported on Figure 2. It is important to note that for all the copper sulfides mentioned in this study, copper is monovalent including CuS compounds such as covellite presented in Figure 2. The Agri-1 site was selected as being representative of the Cu speciation pattern of the all the other sites. The spectra of reference compounds exhibited different characteristic features depending on Cu oxidation state and symmetry at 8986 eV for CuS and 8996 eV for Cu-malate (dashed lines, Figure 2a).

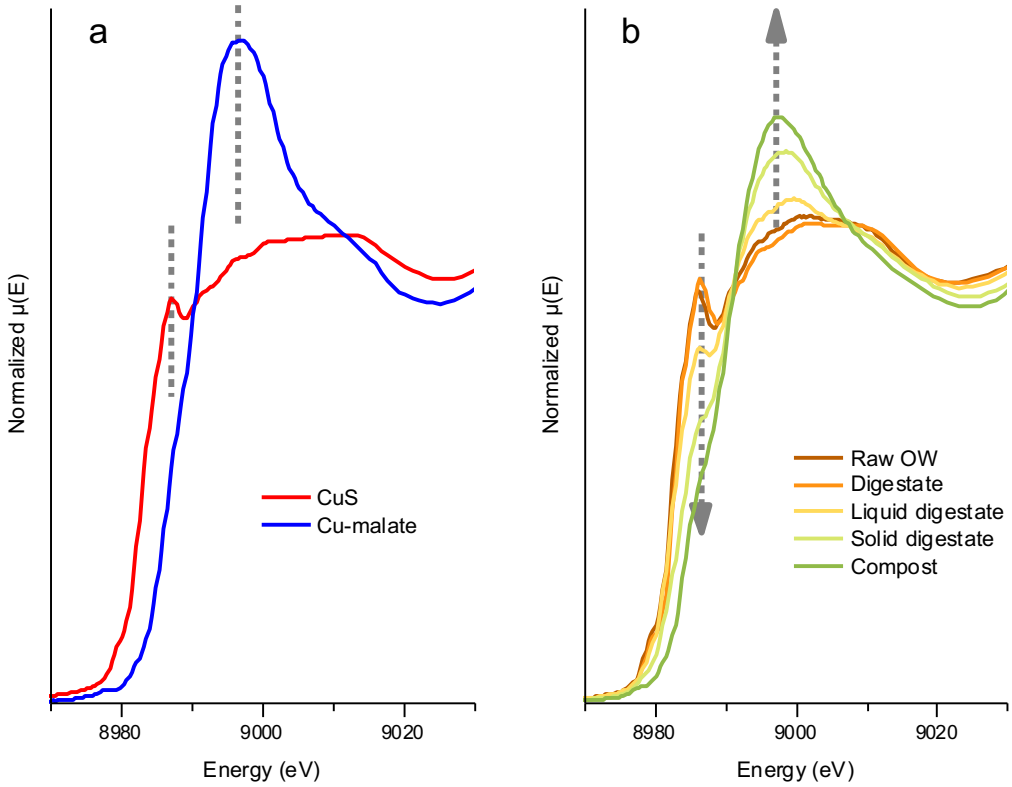

Figure 2: Normalized Cu K-edge XANES spectra of (a) references and (b) raw and treated OWs at different treatment steps at the Agri-1 site. Dashed lines correspond to characteristic features of reference compounds (8986 eV for nano-CuS and 8996 eV for Cu-malate) and dashed arrows indicate spectral changes along OW treatment.

For the OW samples, Cu oxidation state evolved during the different treatment steps (Figure 2b). XANES spectra of raw OW and digestate are close to the spectrum of the nano-Cu(I)S reference. After separation of solid/liquid fractions of digestate, the liquid digestate speciation was modified compared to that of the digestate: the intensity of the peak at 8986 eV decreased while a new maximum at 8996 eV appeared. This trend continued evolving for the solid digestate and then the compost, whose spectrum was very similar to that of the Cu(II)-malate compound reference.

In addition to this visual inspection of the XANES spectra pattern, linear combination fitting (LCF) was performed to obtain quantitative results on Cu oxidation state along the treatment (Figure 1b). LCF

results confirmed that Cu(I) was the major oxidation state in raw OWs ranging from 88 to 100%, regardless of their origin (i.e., urban, agricultural or central). Copper oxidation state pattern can be explained by the physical-chemical conditions during storage and treatment. Indeed, the low dry matter content of raw OWs favors reducing conditions (oxidation reduction potential (ORP) values ranged from -213 to -138 mV[23]) and hence the formation of Cu(I) species (see Figure SI-1a).[9]

When compared to raw OWs, AD did not cause any change in the Cu oxidation state. Indeed, the range of Cu(I) present in digestate samples remained in the range 88-100%. The more reducing conditions in digestates (ORP = -249 to -243mV) compared with raw OWs contributed to maintain the Cu(I) oxidation state.

The solid fractions of digestate from Urban-1, Agri-1 and Central-1 included a majority of Cu(I) (from 56 to 87%), but also a significant contribution of Cu(II) (from 44 to 13%). After separation, the solid fractions of digestate from Agri-1 and Central-1 were stockpiled and had been exposed to the atmosphere for some days before sampling and hence a fraction of Cu(I) may have been oxidized. For Urban-2 and Central-2, no significant change of oxidation state was observed comparing the digestates with their solid fraction counterparts. These solid fractions of digestates were sampled directly at the end of the separation process and exposure to the atmosphere was thus limited.[23]

In composts, Cu(II) became the major oxidation state in Agri-1 (100%) and Urban-2 (64%) and increased up to 46% in compost from Urban-1. Oxidizing conditions were favoured during the composting aerobic process, confirming previous observations for composted biosolid. [10, 12]

In summary, XANES analysis indicated that the Cu oxidation state was subjected to changes along the OW treatment process, mostly depending on the anaerobic/aerobic conditions prevailing in each treatment stage. It can thus be expected that such changes were also reflected in transformations in the molecular environment of Cu, involving *e.g.* Cu minerals or organic/inorganic bearing phases with distinct environmental behaviour. This was assessed using EXAFS and is presented and discussed next.

Changes in Cu bearing phases along OW treatment

A visual inspection of the Cu K-edge EXAFS spectra and respective Fourier transforms of raw and treated OWs (shown in Figure SI-2) revealed transformations in the Cu speciation along the different treatment stages: from a reduced, sulfurized species in raw OW and digestate to an oxidized, complexed by organic moieties in compost. The proportion of each Cu species present in raw and treated OWs assessed via the LCF procedure for the Cu K-edge EXAFS spectrum of each sample is presented in Figure 1c.

Cu(I)-sulfides (nano-Cu_xS and Cu_2S, SI-4) accounted for 100% of the Cu species in the raw OWs and digestates, with a single exception for the raw OW from Central-2 where 24% Cu-citrate was detected. These results are in line with previous studies that showed that Cu(I)-sulfides was the main species in pig slurries and sewage sludge.[8, 9, 15, 17] Lower proportion of Cu(I)-sulfides (from 16 to 52%) were also previously reported for raw OWs and digestates. These rather contrasting results might be attributed to different sampling and storage procedures.[14] Indeed, it has been demonstrated that OWs samples ageing in ambient conditions, even after freeze-drying, quickly altered the speciation of nano-ZnS initially present[23], which could also be expected for Cu(I)-sulfides. Here, the samples were maintained frozen after freeze-drying to preserve initial speciation (section standard bulk XAS analysis).

Cu(II) species were completely absent in the digestates. However, they were detected in the liquid and/or solid fraction of digestates of Urban-1, Agri-1 and Central-1, accounting for 15 to 66% of Cu speciation. Cu-citrate was the main oxidized species (ranging from 15 to 65%) and Cu-carbonate was only detected in the solid digestate of Agri-1, at 13%. In composts, Cu speciation differed drastically from Cu speciation in digestates (Urban-1, Urban-2 and Agri-1) or in raw OWs (Urban-3). Indeed, nano-Cu_xS accounted for less than 40% of Cu speciation whereas Cu-citrate and amorphous Cu-phosphate accounted for 60 to 100% of Cu speciation. During composting, the oxidative dissolution of nano-Cu_xS species release Cu^{2+} likely to be complexed by organic compounds and/or precipitated with phosphate as previously detected in aged and composted biosolids [10, 12] or municipal solid waste compost. [13]

It is worth noting that LCF results were fully consistent comparing XANES and EXAFS approaches. Indeed, the proportion of redox species Cu(I) and Cu(II) based on XANES LCF (Figure 1b) agreed with the proportion of the Cu species derived from EXAFS LCF (Figure 1c). Moreover, the transformations of Cu species described here along the OW treatment process were independent of the origin of the OWs (i.e., urban, agricultural, or central).

Standard bulk XAS techniques provide an average global response and do not address the Cu speciation heterogeneity. In the next section, we compared the spatial heterogeneity of Cu species in OWs at the µm scale with standard bulk XAS techniques.

Spatial heterogeneity of Cu species in OWs

Micro-X-ray fluorescence microscopy (µ-XRF) chemical mapping enabled characterization of the spatial distribution of elements (Figure 3a). For the Urban-3 compost, where bulk XANES and EXAFS indicated a mixture of Cu(I) and Cu(II) species (Figure 1), Cu (red in tricolor µXRF map) was present in large particles of about 100 µm as well as in numerous spots smaller than 10 µm distributed over the whole map. The Cu co-localization with other elements (e.g. S or Fe) was more difficult to characterise as no clear trend was detected. Instead, the spatial distribution of Cu species was assessed using XANES mapping (Figure 3b). Five clusters were identified for the Urban-3 compost. The average spectra of each cluster are presented in Figure 3c together with two reference compounds: CuS (representative of Cu(I) bound to S) and Cu-malate (representative of Cu(II) bound to O,N). Features A (8986 eV) and B (8996 eV) were observed in all cluster spectra, suggesting the presence of both Cu(I) bound to S (Cu(I)-S) and Cu(II) bound to O,N (Cu(II)-O,N) in all the clusters. This was confirmed by the quantitative LCF results for each cluster spectra shown in Figure 3c. However, the proportions of Cu(I)-S varied from 10% (purple cluster 4) to 84% (brown cluster 5) and the proportion of Cu(II)-O,N from 16% to 90%. The surface area of each cluster was quantified based on the number of pixels where each cluster lied. Noteworthy, the blue cluster was detected in 221 156 pixels, accounting for 80% of the scanned surface. By combining the surface area of each cluster with its respective speciation, it was estimated that Cu(I)-S accounted for 35% and Cu(II)-O,N for 65% of Cu speciation in the whole XANES map of Urban-3 compost.

The same approach conducted for the Urban-3 compost (Figure 3) was repeated for the Urban-3 raw OW. In addition, samples from Agri-1 (raw OW, digestate, and compost) and Central-1 (raw OW and digestate) were also considered (Figure 4b and SI-5) to provide an overview of different types of OWs. XANES map analysis revealed 7–8% of Cu(II)-O,N in Urban-3 raw OW, Agri-1 raw OW and Agri-1 digestate. This species was not detected by the standard XANES methods (Figure 4a). The presence of Cu(II)-O,N in these OWs was surprising given the redox conditions favorable to the formation of reduced Cu species (ORP = -172 mV and -233 mV for raw and digestate, respectively[23]). Interestingly, Cu(II)-O,N species did not appear as individual cluster or particles. Instead, they were always associated

with reduced Cu(I)-S species in the same cluster. Thus, we can assume that Cu(II) species were embedded into larger Cu(I) sulfides that preserved them from reduction during storage or digestion processes. This 'protection hypothesis' could explain why the Cu(II)-O,N proportion in the Agri-1 raw OW (7 %) was maintained (at 8 %) even when this OW was subjected to increased reducing conditions during AD.

Cu(II)-O,N was also detected in the raw OW and digestate from Central-1, but at very small proportion: 0.1 and 0.01% respectively. This minor Cu(II)-O,N contribution in Agri-1 raw OW, digestate and Urban-3 raw OW could be the result of Cu oxidation caused by constraints during sample shipment and analysis. Indeed, the OWs were first gamma treated to be imported in Australia. During the 2 weeks of this operation, the freeze-dried OWs were stored under ambient conditions whereas they were stored at -20 °C before conventional XAS analysis. In addition, OWs were not protected from atmosphere during the XANES map acquisition, whereas they were placed into a cryostat (Helium temperature) for the conventional bulk XAS spectroscopy.

However, the detection of minor species for five out of the seven OWs studied here highlights the advantages of such spatially resolved spectroscopy while it remains difficult to conclude on the origin of these minor species ('protection hypothesis' and/or partial oxidation during data acquisition). It is worth noting that Cu(I)-S was always detected in association with Cu(II)-O,N, regardless of the studied OWs. In other words, the spatial resolution (2x2 μm^2) does not allow us to resolve these two chemical species, which appeared mixed at this scale. This limits our understanding of the interaction of these species within particles and also the mechanisms of reduction or oxidation during treatment (AD, composting). To overcome the spatial limitation of the analytical techniques, the characterization of chemical species at sub-micrometer scale are needed. The recent combination of nano-focusing optics (e.g. Fresnel zone plates) with coherent diffraction imaging analysis (Ptychography) are triggering new state-of-the-art scanning X-ray nanoprobes aiming to reach down to 10 nm spatial resolution and should allow to address these analytical challenge.

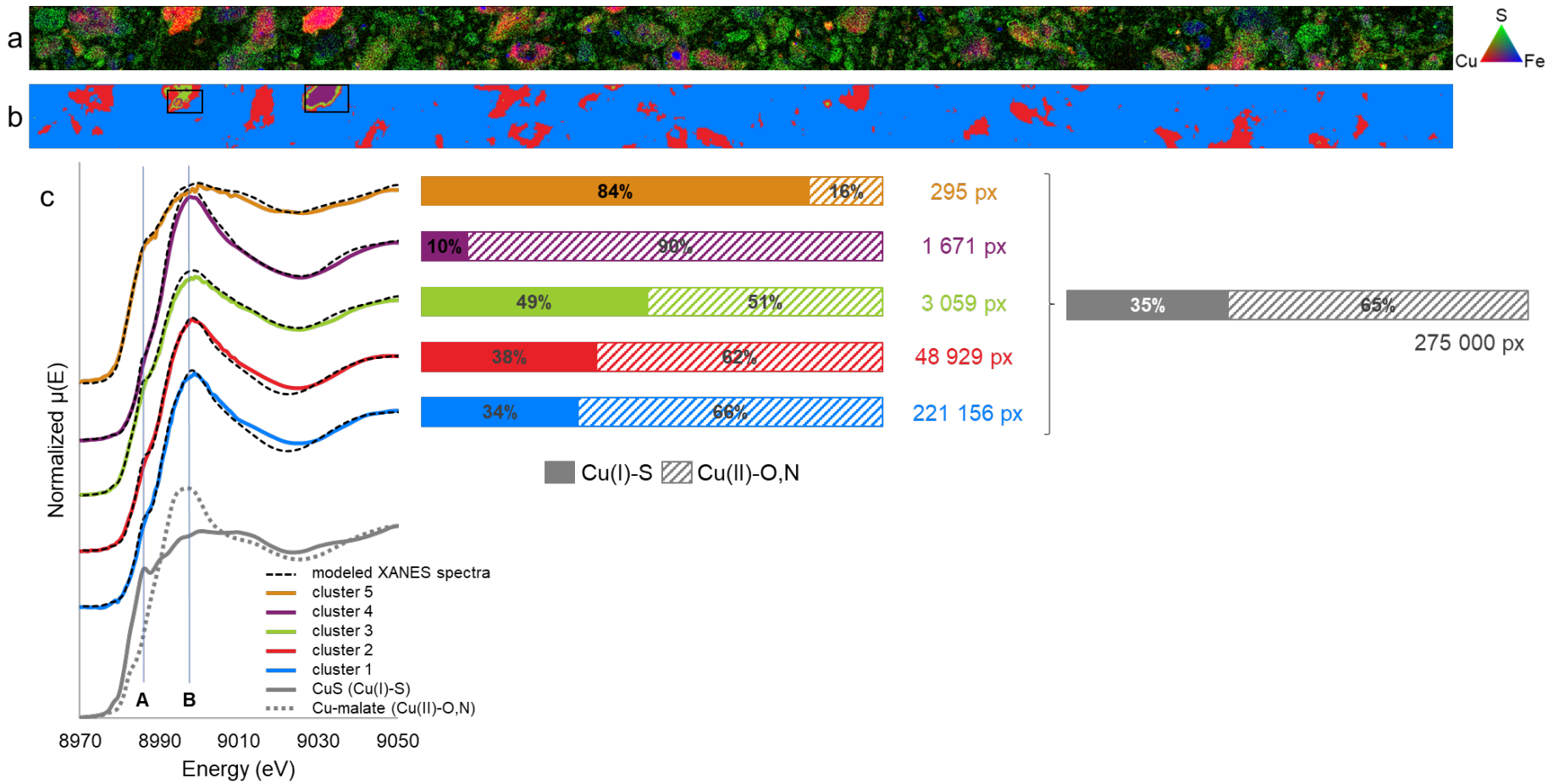

Figure 3: (a) Tricolor μ-XRF map of Cu (red), S (green) and Fe (blue) distribution in the Urban-3 compost. (b) Cluster analysis of the Cu K-edge XANES map with color coding for the 5 clusters. The map size is 5x0.22 mm² (pixel size: 2x2 μm², total number of pixels: 275 000). (c) Normalized cluster (color-coded) and modelled (dotted, black) Cu K-edge XANES spectra (left) ; Cu speciation determined from the linear combination fitting (LCF) of XANES spectra of each cluster and their corresponding pixel number on map (b) (middle) ; Cu speciation calculated for the whole Cu K-edge XANES map using the Cu speciation of the XANES spectra of the 5 clusters and weighted by corresponding number of pixels (right).

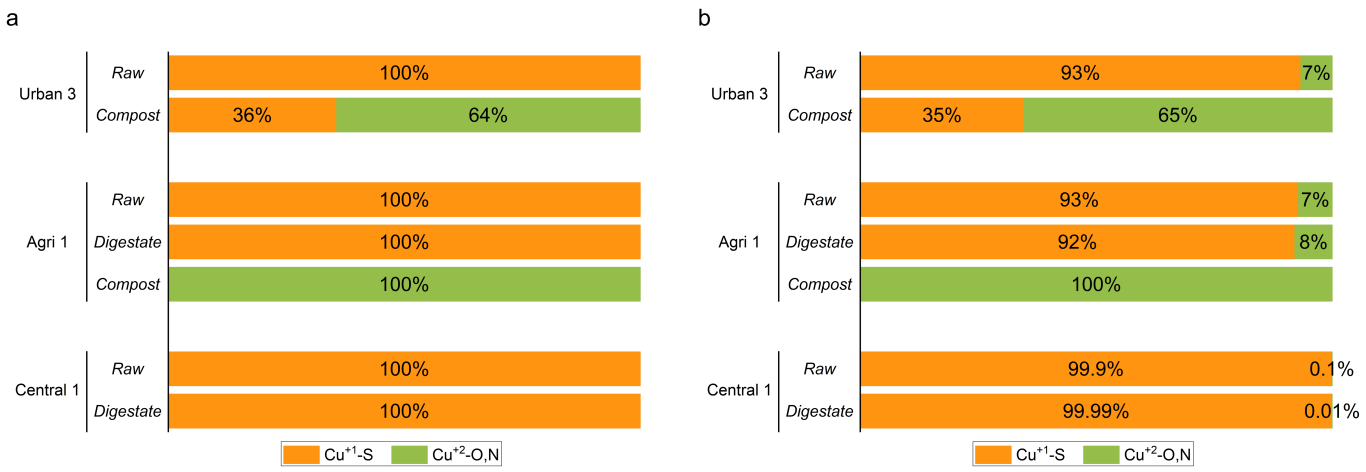

Figure 4: Comparison of Cu speciation of raw and treated OWs determined from the LCF of (a) the standard bulk Cu K-edge XANES spectra and (b) the cluster spectra derived from the PCA and cluster analyses of the Cu K-edge XANES map.

Contrasted Cu and Zn speciation patterns in OWs

Together with Cu, Zn is also an important contaminant present in OWs.[23] However, the pattern of Cu species reported here reveal considerable differences compared to that of Zn[23] in the same set of OW samples. For 20 out of the 22 OWs analysed here, the proportion of Cu(I)-sulfide was higher than that of nano-sized Zn-sulfide (nano-ZnS). Indeed, Cu(I)-sulfide was the major species in raw OWs regardless of the DM content, whereas nano-ZnS was a major species in raw liquid OWs and a minor species in raw OWs with high DM content. Since Cu(I)-sulfide largely prevailed in raw OWs, AD little affected the Cu speciation, which was mostly preserved as Cu(I)-sulfide. Differently, AD always favored the formation of nano-ZnS (71-100% of Zn in digestates compared to 11-90% of Zn in raw OWs before AD).

The differences highlighted above could be explained by the higher affinity of Cu for sulfur compared to Zn.[38] In addition, different reduced Cu(I) species (Cu_2S and nano-Cu_xS) behaved differently from one to another. XANES showed that reduced Cu(I) species prevailed in the six raw OWs analysed (≥ 88 %) and that these high proportions were maintained after AD (Figure 1b). However, EXAFS showed that reduced Cu(I) species could consist of either nano-Cu_xS or Cu_2S. When Cu_2S prevailed in raw OWs (67 % in Agri-1 and 77 % in Central-1) over nano-Cu_xS, very similar proportions of Cu_2S were present in the respective digestates. Differently, when nano-Cu_xS prevailed in raw OWs (52–64 % in the three urban OWs and 76 % in Central-2), this proportions decreased in the respective digestates, and additional Cu_2S was formed (Figure 1c). The parallel can be drawn with studies that have described the ageing of amorphous Cu_xS_{prim} to covellite (crystalline CuS) and the sulfidation of copper oxide nanoparticles.[39-41] Indeed, mixing Cu and sulfur soluble salts in aqueous solutions resulted in the formation of an amorphous (primitive) co-precipitate of Cu_xS that was mestastable and aged quickly (24h at 20°C, 35 min at 50°C) to a structure with the characteristics of covellite (crystalline CuS). [30, 41, 42] Similarly, CuO nanoparticles were rapidly sulfidized and first transformed into amorphous Cu_xS that gradually evolved into crystalline CuS. Furthermore, it has been shown that under anoxic conditions, organic matter limits the growth of Cu_xS particles to 50 nm, and these Cu_xS nanoparticles are stable and not dissolved. But upon ageing in the presence of oxygen and organic matter, a structural evolution of these Cu_xS nanoparticles is observed with the growth of crystalline domains consisting of covellite (CuS).[43] Consequently, we can assume that the reducing conditions, the high sulfur and organic matter content in raw OWs are favorable for the formation of nano-Cu_xS, as indicated in Figure 1. Then, the combination of anoxic storage of raw OWs with the AD likely contribute to nano-Cu_xS particles ageing and hence the higher proportion of crystallized Cu sulfide detected in digestates. In contrast, nano-ZnS in raw OWs and digestates did not transform into crystalline ZnS. This different pattern is likely the reason of the discrepancies between Cu and Zn speciation in raw OWs and digestates.

In composts, nano-ZnS was minor (< 10%) and Zn was mostly present as amorphous Zn-phosphate and Zn sorbed to ferrihydrite. On the other hand, 20 to 40% of Cu(I)-sulfide was detected in three out of four composts analysed here. Accordingly, Donner et al.[10] reported that Cu-sulfides were persistent in aged biosolids (i.e., stockpiled, composted) whereas Zn-sulfides were not detected anymore. In soil, Hesterberg et al. [20] had also observed that Zn-sulfides oxidized more rapidly than Cu-sulfides. Galvanic protection was evoked to explain this behaviour [20]: Cu-sulfide with a higher oxidation phase-boundary potential acts as cathodic to Zn-sulfide accelerating the oxidation of the latter.[44] For galvanic protection, Cu- and Zn-sulfides need to be mixed in close spatial proximity[20] which is consistent with the co-location of Cu, Zn and S previously observed in raw pig slurry.[45]

This study provides general trends about the Cu speciation in raw and treated OWs. However, further research is needed to determine the fate of Cu following OW soil application. Indeed, in soil the stability of nanosized Cu(I)-sulfide is likely different from that of crystallized Cu_2S, and Cu bound to organic matter in compost is likely released due to organic matter mineralization. It is therefore

essential to study this fate to improve our capacity to predict the ecotoxicological impact of agricultural OW recycling.

References

(1) Nicholson, F. A.; Smith, S. R.; Alloway, B. J.; Carlton-Smith, C.; Chambers, B. J. An inventory of heavy metals inputs to agricultural soils in England and Wales. *Science of The Total Environment* **2003**, *311* (1-3), 205-219.
(2) Belon, E.; Boisson, M.; Deportes, I. Z.; Eglin, T. K.; Feix, I.; Bispo, A. O.; Galsomies, L.; Leblond, S.; Guellier, C. R. An inventory of trace elements inputs to French agricultural soils. *Science of the Total Environment* **2012**, *439*, 87-95. DOI: 10.1016/j.scitotenv.2012.09.011.
(3) Luo, L.; Ma, Y.; Zhang, S.; Wei, D.; Zhu, Y.-G. An inventory of trace element inputs to agricultural soils in China. *Journal of Environmental Management* **2009**, *90* (8), 2524-2530. DOI: http://dx.doi.org/10.1016/j.jenvman.2009.01.011.
(4) Fairbrother, A.; Wenstel, R.; Sappington, K.; Wood, W. Framework for Metals Risk Assessment. *Ecotoxicology and Environmental Safety* **2007**, *68* (2), 145-227. DOI: https://doi.org/10.1016/j.ecoenv.2007.03.015.
(5) Li, B.; Zhang, X.; Tefsen, B.; Wells, M. From speciation to toxicity: Using a "Two-in-One" whole-cell bioreporter approach to assess harmful effects of Cd and Pb. *Water Research* **2022**, *217*, 118384. DOI: https://doi.org/10.1016/j.watres.2022.118384.
(6) Uchimiya, M.; Bannon, D.; Nakanishi, H.; McBride, M. B.; Williams, M. A.; Yoshihara, T. Chemical Speciation, Plant Uptake, and Toxicity of Heavy Metals in Agricultural Soils. *Journal of Agricultural and Food Chemistry* **2020**, *68* (46), 12856-12869. DOI: 10.1021/acs.jafc.0c00183.
(7) Li, L.; Hu, L.; Zhou, Q.; Huang, C.; Wang, Y.; Sun, C.; Jiang, G. Sulfidation as a Natural Antidote to Metallic Nanoparticles Is Overestimated: CuO Sulfidation Yields CuS Nanoparticles with Increased Toxicity in Medaka (Oryzias latipes) Embryos. *Environmental Science & Technology* **2015**, *49* (4), 2486-2495. DOI: 10.1021/es505878f.
(8) Formentini, T. A.; Basile-Doelsch, I.; Legros, S.; Frierdich, A. J.; Pinheiro, A.; Fernandes, C. V. S.; Mallmann, F. J. K.; Borschneck, D.; da Veiga, M.; Doelsch, E. Copper (Cu) speciation in organic-waste (OW) amended soil: Instability of OW-borne Cu(I) sulfide and role of clay and iron oxide minerals. *Science of The Total Environment* **2022**, *848*, 157779. DOI: https://doi.org/10.1016/j.scitotenv.2022.157779.
(9) Legros, S.; Chaurand, P.; Rose, J.; Masion, A.; Briois, V.; Ferrasse, J. H.; Saint Macary, H.; Bottero, J. Y.; Doelsch, E. Investigation of Copper Speciation in Pig Slurry by a Multitechnique Approach. *Environmental Science & Technology* **2010**, *44* (18), 6926-6932. DOI: 10.1021/es101651w.
(10) Donner, E.; Howard, D. L.; de Jonge, M. D.; Paterson, D.; Cheah, M. H.; Naidu, R.; Lombi, E. X-ray Absorption and Micro X-ray Fluorescence Spectroscopy Investigation of Copper and Zinc Speciation in Biosolids. *Environmental Science & Technology* **2011**, *45* (17), 7249-7257. DOI: 10.1021/es201710z.
(11) Tella, M.; Legros, S.; Monteiro, A. N. T. R.; Forouzandeh, A.; Penen, F.; Durosoy, S.; Doelsch, E. Unexpected Cu and Zn speciation patterns in the broiler feed-animal-excreta system revealed by XAS spectroscopy. *Chemosphere* **2023**, *340*, 139684. DOI: https://doi.org/10.1016/j.chemosphere.2023.139684.
(12) Donner, E.; Ryan, C. G.; Howard, D. L.; Zarcinas, B.; Scheckel, K. G.; McGrath, S. P.; de Jonge, M. D.; Paterson, D.; Naidu, R.; Lombi, E. A multi-technique investigation of copper and zinc distribution, speciation and potential bioavailability in biosolids. *Environ Pollut* **2012**, *166* (0), 57-64. DOI: 10.1016/j.envpol.2012.02.012.
(13) Tella, M.; Bravin, M. N.; Thuriès, L.; Cazevieille, P.; Chevassus-Rosset, C.; Collin, B.; Chaurand, P.; Legros, S.; Doelsch, E. Increased zinc and copper availability in organic waste amended soil potentially involving distinct release mechanisms. *Environ Pollut* **2016**, *212*, 299-306. DOI: http://dx.doi.org/10.1016/j.envpol.2016.01.077.
(14) Legros, S.; Levard, C.; Marcato-Romain, C.-E.; Guiresse, M.; Doelsch, E. Anaerobic Digestion Alters Copper and Zinc Speciation. *Environmental Science & Technology* **2017**, *51* (18), 10326-10334. DOI: 10.1021/acs.est.7b01662.
(15) Wang, Q.; Zhang, C.; Jung, H.; Liu, P.; Patel, D.; Pavlostathis, S. G.; Tang, Y. Transformation and Mobility of Cu, Zn, and Cr in Sewage Sludge during Anaerobic Digestion with Pre- or Interstage

Hydrothermal Treatment. *Environmental Science & Technology* **2021**, *55* (3), 1615-1625. DOI: 10.1021/acs.est.0c05164.
(16) Wielinski, J.; Gogos, A.; Voegelin, A.; Müller, C.; Morgenroth, E.; Kaegi, R. Transformation of Nanoscale and Ionic Cu and Zn during the Incineration of Digested Sewage Sludge (Biosolids). *Environmental Science & Technology* **2019**, *53* (20), 11704-11713. DOI: 10.1021/acs.est.9b01983.
(17) Cheng, Y.; Luo, L.; Lv, J.; Li, G.; Wen, B.; Ma, Y.; Huang, R. Copper Speciation Evolution in Swine Manure Induced by Pyrolysis. *Environmental Science & Technology* **2020**, *54* (14), 9008-9014. DOI: 10.1021/acs.est.9b07332.
(18) Gräfe, M.; Donner, E.; Collins, R. N.; Lombi, E. Speciation of metal(loid)s in environmental samples by X-ray absorption spectroscopy: A critical review. *Analytica Chimica Acta* **2014**, *822* (0), 1-22. DOI: http://dx.doi.org/10.1016/j.aca.2014.02.044.
(19) Manceau, A.; Marcus, M. A.; Tamura, N. Quantitative speciation of heavy metals in soils and sediments by synchrotron X-ray techniques. In *Applications of Synchrotron Radiation in Low-Temperature Geochemistry and Environmental Science*, P. Fenter, P., Sturchio, N. C. Eds.; Reviews in Mineralogy and Geochemistry, Vol. 49; Mineralogical Society of America, 2002; pp 341-428.
(20) Hesterberg, D.; Duff, M. C.; Dixon, J. B.; Vepraskas, M. J. X-ray Microspectroscopy and Chemical Reactions in Soil Microsites. *Journal of Environmental Quality* **2011**, *40* (3), 667-678. DOI: https://doi.org/10.2134/jeq2010.0140.
(21) Lombi, E.; de Jonge, M. D.; Donner, E.; Ryan, C. G.; Paterson, D. Trends in hard X-ray fluorescence mapping: environmental applications in the age of fast detectors. *Analytical and Bioanalytical Chemistry* **2011**, *400* (6), 1637-1644. DOI: 10.1007/s00216-011-4829-2.
(22) Etschmann, B. E.; Donner, E.; Brugger, J.; Howard, D. L.; de Jonge, M. D.; Paterson, D.; Naidu, R.; Scheckel, K. G.; Ryan, C. G.; Lombi, E. Speciation mapping of environmental samples using XANES imaging. *Environmental Chemistry* **2014**, *11* (3), 341-350. DOI: http://dx.doi.org/10.1071/EN13189.
(23) Le Bars, M.; Legros, S.; Levard, C.; Chaurand, P.; Tella, M.; Rovezzi, M.; Browne, P.; Rose, J.; Doelsch, E. Drastic Change in Zinc Speciation during Anaerobic Digestion and Composting: Instability of Nanosized Zinc Sulfide. *Environmental Science & Technology* **2018**, *52* (22), 12987-12996. DOI: 10.1021/acs.est.8b02697.
(24) Dœlsch, E.; Basile-Dœlsch, I.; Rose, J.; Masion, A.; Borschneck, D.; Hazemann, J.-L.; Saint Macary, H.; Bottero, J.-Y. New combination of EXAFS spectroscopy and density fractionation for the speciation of chromium within an andosol. *Environmental science & technology* **2006**, *40* (24), 7602-7608.
(25) Landrot, G. *Fastosh v. 1.0 - User Manual*; 2021. https://www.synchrotron-soleil.fr/fr/lignes-de-lumiere/samba.
(26) Ravel, B.; Newville, M. ATHENA, ARTEMIS, HEPHAESTUS: data analysis for X-ray absorption spectroscopy using IFEFFIT. *Journal of synchrotron radiation* **2005**, *12* (4), 537-541.
(27) Collin, B.; Doelsch, E.; Keller, C.; Cazevieille, P.; Tella, M.; Chaurand, P.; Panfili, F.; Hazemann, J.-L.; Meunier, J.-D. Evidence of sulfur-bound reduced copper in bamboo exposed to high silicon and copper concentrations. *Environ Pollut* **2014**, *187*, 22-30. DOI: https://doi.org/10.1016/j.envpol.2013.12.024.
(28) Schlegel, M. L.; Manceau, A. Binding mechanism of Cu(II) at the clay-water interface by powder and polarized EXAFS spectroscopy. *Geochimica Et Cosmochimica Acta* **2013**, *113*, 113-124. DOI: 10.1016/j.gca.2013.03.019.
(29) Guigues, S.; Bravin, M. N.; Garnier, C.; Masion, A.; Chevassus-Rosset, C.; Cazevieille, P.; Doelsch, E. Involvement of nitrogen functional groups in high-affinity copper binding in tomato and wheat root apoplasts: spectroscopic and thermodynamic evidence†. *Metallomics* **2016**, *8* (3), 366-376. DOI: 10.1039/c5mt00298b (acccessed 9/8/2023).
(30) Pattrick, R. A. D.; Mosselmans, J. F. W.; Charnock, J. M.; England, K. E. R.; Helz, G. R.; Garner, C. D.; Vaughan, D. J. The structure of amorphous copper sulfide precipitates: An X-ray absorption study. *Geochimica et Cosmochimica Acta* **1997**, *61* (10), 2023-2036. DOI: http://dx.doi.org/10.1016/S0016-7037(97)00061-6.
(31) Ryan, C. G.; Siddons, D. P.; Kirkham, R.; Li, Z. Y.; de Jonge, M. D.; Paterson, D. J.; Kuczewski, A.; Howard, D. L.; Dunn, P. A.; Falkenberg, G.; et al. Maia X-ray fluorescence imaging: Capturing detail in

complex natural samples. *Journal of Physics: Conference Series* **2014**, *499* (1), 012002. DOI: 10.1088/1742-6596/499/1/012002.
(32) Lerotic, M.; Mak, R.; Wirick, S.; Meirer, F.; Jacobsen, C. MANTiS: a program for the analysis of X-ray spectromicroscopy data. *Journal of Synchrotron Radiation* **2014**, *21* (5), 1206-1212. DOI: doi:10.1107/S1600577514013964.
(33) Lerotic, M.; Jacobsen, C.; Gillow, J. B.; Francis, A. J.; Wirick, S.; Vogt, S.; Maser, J. Cluster analysis in soft X-ray spectromicroscopy: Finding the patterns in complex specimens. *Journal of Electron Spectroscopy and Related Phenomena*

Proceeding of the Fourteenth International Conference on Vacuum Ultraviolet Radiation Physics **2005**, *144-147*, 1137-1143.
(34) Lerotic, M.; Jacobsen, C.; Schafer, T.; Vogt, S. Cluster analysis of soft X-ray spectromicroscopy data. *Ultramicroscopy* **2004**, *100* (1-2), 35-57.
(35) Tella, M.; Doelsch, E.; Letourmy, P.; Chataing, S.; Cuoq, F.; Bravin, M. N.; Saint Macary, H. Investigation of potentially toxic heavy metals in different organic wastes used to fertilize market garden crops. *Waste Management* **2013**, *33* (1), 184-192. DOI: http://dx.doi.org/10.1016/j.wasman.2012.07.021.
(36) Inglezakis, V. J.; Zorpas, A. A.; Karagiannidis, A.; Samaras, P.; Voukkali, I.; Sklari, S. European Union legislation on sewage sludge management. *Fresenius Environmental Bulletin* **2014**, *23* (2A), 635-639, Article.
(37) Le Bars, M.; Levard, C.; Legros, S.; Vidal, V.; Fernandez-Martinez, A.; Michel, F. M.; Thill, A.; Prelot, B.; Dublet-Adli, G.; Borschneck, D.; et al. Size and Strain of Zinc Sulfide Nanoparticles Altered by Interaction with Organic Molecules. *Environmental Science & Technology* **2022**, *56* (23), 16831-16837. DOI: 10.1021/acs.est.2c05268.
(38) Myers, R. J. The new low value for the second dissociation constant for H2S: Its history, its best value, and its impact on the teaching of sulfide equilibria. *Journal of Chemical Education* **1986**, *63* (8), 687. DOI: 10.1021/ed063p687.
(39) Gogos, A.; Thalmann, B.; Voegelin, A.; Kaegi, R. Sulfidation kinetics of copper oxide nanoparticles. *Environmental Science: Nano* **2017**, *4* (8), 1733-1741, 10.1039/C7EN00309A. DOI: 10.1039/C7EN00309A.
(40) Ma, R.; Stegemeier, J.; Levard, C.; Dale, J. G.; Noack, C. W.; Yang, T.; Brown, G. E.; Lowry, G. V. Sulfidation of copper oxide nanoparticles and properties of resulting copper sulfide. *Environmental Science: Nano* **2014**, *1* (4), 347-357, 10.1039/C4EN00018H. DOI: 10.1039/C4EN00018H.
(41) Luther, G. W.; Theberge, S. M.; Rozan, T. F.; Rickard, D.; Rowlands, C. C.; Oldroyd, A. Aqueous Copper Sulfide Clusters as Intermediates during Copper Sulfide Formation. *Environmental Science & Technology* **2002**, *36* (3), 394-402. DOI: 10.1021/es010906k.
(42) Shea, D.; Helz, G. R. Solubility product constants of covellite and a poorly crystalline copper sulfide precipitate at 298 K. *Geochimica et Cosmochimica Acta* **1989**, *53* (2), 229-236. DOI: https://doi.org/10.1016/0016-7037(89)90375-X.
(43) Hoffmann, K.; Bouchet, S.; Christl, I.; Kaegi, R.; Kretzschmar, R. Effect of NOM on copper sulfide nanoparticle growth, stability, and oxidative dissolution. *Environmental Science: Nano* **2020**, *7* (4), 1163-1178, 10.1039/C9EN01448A. DOI: 10.1039/C9EN01448A.
(44) Sato, M. Persistency-field Eh-pH diagrams for sulfides and their application to supergene oxidation and enrichment of sulfide ore bodies. *Geochimica et Cosmochimica Acta* **1992**, *56* (8), 3133-3156. DOI: https://doi.org/10.1016/0016-7037(92)90294-S.
(45) Legros, S.; Doelsch, E.; Masion, A.; Rose, J.; Borshneck, D.; Proux, O.; Hazemann, J. L.; Saint-Macary, H.; Bottero, J. Y. Combining Size Fractionation, Scanning Electron Microscopy, and X-ray Absorption Spectroscopy to Probe Zinc Speciation in Pig Slurry. *Journal of Environmental Quality* **2010**, *39* (2), 531-540. DOI: 10.2134/jeq2009.0096.